

Measurements of collisional properties of spheres using high-speed video analysis

Laurent Labous,* Anthony D. Rosato, and Rajesh N. Dave

Particle Technology Center, New Jersey Institute of Technology, University Heights, Newark, New Jersey 07102

(Received 30 May 1997)

In this paper we report measurements of collisional properties of spheres using high-speed video analysis. These results agree with a simple collision operator. We study the size and velocity dependences of the coefficient of restitution in the normal direction. The experimental data are compared with the relevant models of energy dissipation and show the existence of two dissipation regimes. For large impact velocities a plastic deformation model is in good agreement with our measurements, while for smaller velocities a model of viscoelastic dissipation gives qualitative agreement.

[S1063-651X(97)01011-8]

PACS number(s): 82.20.Wt, 46.10.+z, 62.20.Fe, 83.70.Fn

I. INTRODUCTION

Bulk solids or granular materials are assemblies of discrete solid particles. They exhibit very complex and diverse static or dynamic behaviors. Because bulk solids occupy a preponderant situation in human activities and environment, they have motivated, in recent years, significant research efforts. Attention has been focused on microstructural level studies that in turn should allow for quantitative predictions of large scale flows. Hence, more fascinating phenomena have been intensively studied [1].

Computer simulations of granular flows have proved to be a powerful investigation tool to test and validate theoretical models but also to complement and interpret experimental findings. In the simulations the individual components, most of the times idealized as disks or spheres, of the material interact through binary collisions. Collisions are “solved” using prescribed force schemes for soft-sphere (molecular dynamics) [2–8] simulations and collision operators for hard-spheres (event-driven) simulations [9–17]. With molecular dynamics one integrates timewise Newton’s equation for each particle, while event-driven techniques process from one collision to the next, and obtain the postcollisional particle kinematics as a function of precollisional values and of the parameters defining the operator. Because binary interactions govern the transport properties of rapid or agitated granular flows through conversion of the macroscopic kinetic energy into fluctuation energy, the specific contact laws are fundamental [3,7,8,18,19] and constitute a keystone of simulations as well as theories. It is therefore crucial to have a knowledge beforehand of the properties of the flow material and to be able to mimic the actual rheological behaviors.

In recent years this issue has been very controversial. A basic requirement of numerical simulations as well as theories is that the interaction model used be sufficiently simple to guarantee numerical efficiency or allow for tractable calculations. Many collision models have been proposed (see Ref. [20] and references therein) that all are more or less

reductive simplifications of real collision processes and do not always rely on well established experimental knowledge or sound theoretical results. From a theoretical point of view the collision between two inelastic frictional spheres is particularly difficult due to complicated mechanisms responsible for energy dissipation [21,22] and to mechanical coupling between normal and tangential deformations [23–25]. On the basis of previous theoretical results due to Landau and Lifshitz [26] for the compression of elastic spheres and to Mindlin [30] for the tangential loading of elastic frictional spheres, Maw *et al.* [24] established a numerical model describing the oblique collision of spheres. In this model dissipation arises due to frictional interaction of the contact surfaces. It is verified experimentally using a flat puck gliding above an air table and colliding with a flat surface. Sondergaard and Chaney [29] also studied the collision of a disk with a flat plate. Later the experiment of Foerster *et al.* [27] established this model for small spheres in free flight. However because this model cannot reasonably be incorporated in numerical simulations of large assemblies of spheres or disk, Walton [8] introduced a simple collision operator that captures the main features of the oblique collision through the definition of three collisional properties as described in more detail in Sec. II. In such a model, *ad hoc* definitions of the parameters may be introduced so as to reproduce known material properties. It is a good trade-off between the complexity of the phenomena evidenced in [24] and efficiency requirements mentioned above. While the frictional effects are relatively well understood, all other dissipation mechanisms are still poorly documented and are often condensed in a constant coefficient of restitution whose dependence on the size or velocities of the colliding bodies is ignored. Experimentally it is known that the coefficient of restitution decreases with increasing impact velocity [22,28,29] but data providing relevant scaling laws (of mass and velocity dependence) is inexistent or scarce. Kuwabara and Kono [22] proposed a model of viscoelastic dissipation and compared it with experimental results of collisions between two pendula. This model seemed to properly reproduce the velocity dependence of the coefficient of restitution for low dissipation conditions. For higher velocities, when plastic deformation is likely to occur, Johnson [21] shows, on the basis of an energy balance between kinetic energy and energy of plastic

*Present address: Laboratoire des Milieux Désordonnés et Hétérogènes (Tour 22–case 86), Université Pierre et Marie Curie, 4 Place Jussieu, Paris, France.

deformation, that e should decrease more sharply as a power $-1/4$ of the impact velocity. Both models predict different size dependences, an issue that still has to be answered experimentally.

Recently Schäfer *et al.* [20] carried out a critical study of the collision models used in molecular dynamics simulations. From a comparison with the results of Ref. [27] they showed which are the relevant models for standard materials (metals, hard plastics) usually considered and which are unable to reproduce the experimental data. The velocity dependence of the coefficient of restitution also displays substantial differences from one model to the next, sometimes predicting less dissipation for higher impact velocities, which is unphysical for standard materials.

In summary, the problem encountered by physicists involved in modeling granular media is the poor knowledge of interaction laws that should at least mimic obviously more complicated rheological behaviors and allow efficient computation. On the other hand, interpretation of physical experiments and validation of computer simulations and theoretical models require a quantitative knowledge of the properties of the flow materials. In this paper we present an experiment whereby the kinematics of spheres colliding in free flight can be determined using high-speed video analysis, in order to provide such quantitative information. We start by briefly presenting the collisional properties as defined in [8]. We then describe our experimental apparatus and method. We measure collisional properties of plastic spheres according to the collision operator to be defined below. We further investigate the mass and velocity dependences of the coefficient of restitution for normal impacts, which is one of the three properties entering the collision operator. Finally these measurements are directly compared with the relevant models of energy dissipation as discussed above.

II. DEFINITION OF COLLISIONAL PROPERTIES

In this section we present briefly the ‘‘collision operator’’ introduced by Walton in [8]. Subsequently to the work of Mindlin [30] on the oblique contact of frictional spheres, Maw *et al.* [23,24] modeled the collision of two elastic spheres by subdividing their contact patches into a series of concentric annuli, each of them being either in sticking or in sliding motion relative to the same annulus belonging to the other sphere. Solving numerically the equations of elasticity with mixed boundary conditions they evidenced the possibility during a collision of storing and partly retrieving elastic energy stored as tangential deformation of the spheres in the contact region. These results are captured by a simple collision operator due to Walton [8]: the collision is considered as an instantaneous event and three collisional properties are defined relating the precollision and post collision kinematics. These properties are phenomenological constants describing the inelastic and frictional nature of the interactions but also the coupling between translational and rotational relative motion of the colliding spheres. Let us consider two homogeneous spheres with masses m_1 and m_2 , diameters d_1 and d_2 , moments of inertia about their center I_1 and I_2 ($I_i = m_i d_i^2 / 10$) and colliding when their centers lie at \vec{r}_1 and \vec{r}_2 . Prior to the collision the sphere centers have velocities

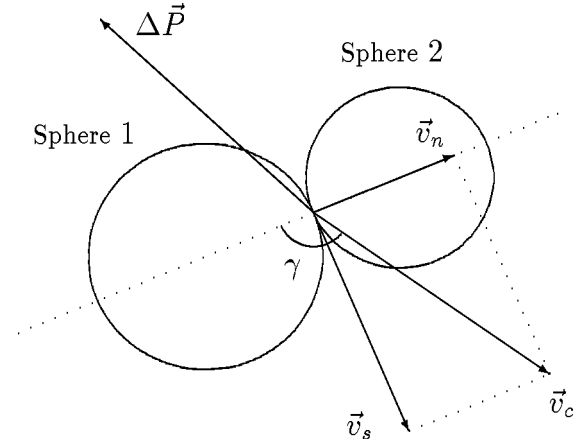


FIG. 1. Relative kinematics of two colliding spheres. $\Delta\vec{P}$ is the impulse exerted by sphere 2 on sphere 1; \vec{v}_c is the relative velocity of the spheres at their contact point.

\vec{v}_1 and \vec{v}_2 and the spheres are spinning with rotation vectors $\vec{\omega}_1$ and $\vec{\omega}_2$. During the collision sphere 2 exerts an impulse $\Delta\vec{P}$ on sphere 1. The new values of velocities and rotation, hereafter denoted with a prime, are obtained from the conservation of linear momentum,

$$\Delta\vec{P} = m_1(\vec{v}'_1 - \vec{v}_1) = -m_2(\vec{v}'_2 - \vec{v}_2), \quad (1)$$

of angular momentum,

$$-\vec{n} \times \Delta\vec{P} = \frac{2I_1}{d_1}(\vec{\omega}'_1 - \vec{\omega}_1) = \frac{2I_2}{d_2}(\vec{\omega}'_2 - \vec{\omega}_2), \quad (2)$$

and from prescribed relations using the collisional properties. In Eq. (2) \vec{n} is the unit vector joining the centers of the two spheres, i.e., $\vec{n} = (\vec{r}_1 - \vec{r}_2) / |\vec{r}_1 - \vec{r}_2|$. The relative velocity of the spheres at their contact point, or sliding velocity, before collision is (see Fig. 1)

$$\vec{v}_c = \vec{v}_1 - \vec{v}_2 - \left(\frac{d_1}{2} \vec{\omega}_1 + \frac{d_2}{2} \vec{\omega}_2 \right) \times \vec{n}. \quad (3)$$

This velocity has a normal component $\vec{v}_n = (\vec{v}_c \cdot \vec{n}) \vec{n}$ and a component lying in the tangential plane $\vec{v}_s = \vec{v}_c - \vec{v}_n$. The normal coefficient of restitution is defined as

$$(\vec{v}'_1 - \vec{v}'_2) \cdot \vec{n} \stackrel{\text{def}}{=} -e (\vec{v}_1 - \vec{v}_2) \cdot \vec{n}. \quad (4)$$

It is a measure of the energy lost in the normal direction of the relative impact motion. The direction of \vec{v}_s is assumed to be unchanged but its modulus is reduced by a factor $|\beta|$ according to

$$\vec{v}'_s \stackrel{\text{def}}{=} -\beta \vec{v}_s. \quad (5)$$

Similarly to e , β is the coefficient of restitution of the tangential or rotational motion. As shown by Maw *et al.* [23], β is a function of the angle of incidence γ , with possible values lying in the range $[-1; 1]$. The angle γ is illustrated in Fig. 1: it is such that $\cot \gamma = v_n / v_s$. With the above definition of Eq. (4) it is straightforward to show, using the conservation of linear momentum given by Eq. (1), that the normal com-

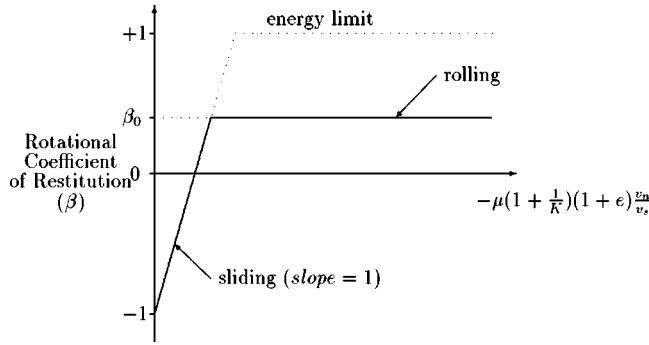


FIG. 2. Variation of the rotational coefficient of restitution β with v_n/v_s as predicted by Eq. (7).

ponent of $\Delta\vec{P}$ is $\Delta\vec{P}_n = -(1+e)m_{\text{red}}\vec{v}_n$ [$m_{\text{red}} = m_1m_2/(m_1+m_2)$ is the reduced mass of the two spheres]. In order to determine the tangential component of momentum change, Walton assumes that a given collision is either *sliding* or *rolling* throughout the contact. In the first case (*sliding*), the tangential component $\Delta\vec{P}_t$ is set equal to its frictional limit according to Coulomb's law: its magnitude $|\Delta\vec{P}_t|$ is a coefficient of friction μ_0 times the magnitude of the normal component $|\Delta\vec{P}_n|$ and it is parallel, but oriented in the opposite direction, to the tangential component of the contact velocity, i.e.,

$$\Delta\vec{P}_t = -\mu_0|\Delta\vec{P}_n|\vec{t}, \quad (6)$$

with $\vec{t} = \vec{v}_s/|\vec{v}_s|$. μ_0 characterizes the frictional properties of the surfaces. For angles of incidence close to π , i.e., nearly head-on collisions, Eq. (6) would yield values of β larger than 1 [8] and thus a net increase of energy. This is why whenever for a given collision the sliding assumption yields a β value greater than β_0 , an *a priori* unknown positive constant smaller than 1, *rolling* is effective. This condition defines a critical angle of incidence γ_0 above which Eq. (6) is no longer valid. In this case, and in the absence of adequate theoretical predictions, β is set equal to this limiting value β_0 . Along with e and μ_0 , β_0 becomes the third unknown collision property we wish to determine from our experiment. It characterizes the restitution, in the tangential motion, of collisions during which rolling in the sense given in [24] occurs. The equations relating the precollisional and postcollisional kinematics of the spheres boil down to [8,4]

$$\beta = \begin{cases} -1 - \mu_0 \left(1 + \frac{1}{K}\right) (1+e) \frac{v_n}{v_s} & \text{for } \gamma \leq \gamma_0 \text{ (sliding)} \\ \beta_0 & \text{for } \gamma \geq \gamma_0 \text{ (rolling),} \end{cases} \quad (7)$$

where $K = 4I/md^2$ is a constant equal to 2/5 for homogeneous spheres. Figure 2 illustrates the variation of β with $-v_n/v_s$ given by Eq. (7). The analysis of a single collision yields the coefficient of normal restitution e , and only one of the two other parameters β_0 and μ_0 . Indeed for a *sliding* contact, β is a function of the angle of approach while μ_0 is now given by the ratio of the tangential to the normal component, usually referred to as the impulse ratio, of the impulse $\Delta\vec{P}$. On the other hand, when *rolling* prevails β is

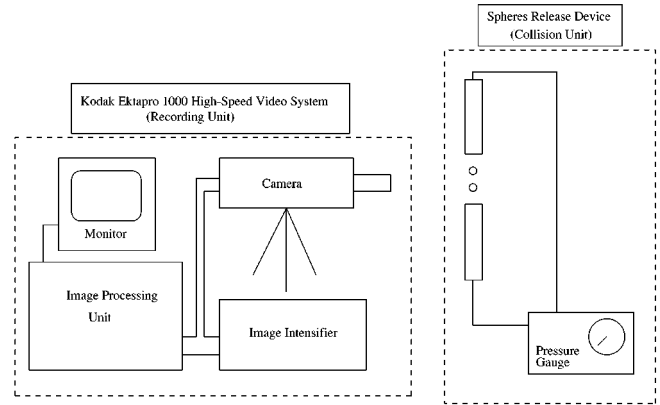


FIG. 3. Experimental setup.

equal to β_0 but the impulse ratio is now varying. Although it is not known *a priori* whether a particular collision will be *rolling* or *sliding*, it is still possible, according to Walton's model, to determine μ_0 and β_0 by producing a plot of β values versus $-v_n/v_s$ values: According to Eq. (7) β_0 is the maximum value taken by β while the slope of the sliding regime is $\mu_0(1+1/K)(1+e)$.

III. EXPERIMENTAL METHODS

Experimental measurements of collision properties of spheres depend entirely on the ability to determine as accurately as possible the kinematics of the two colliding bodies before and after collision. Previous experiments were designed in which either the available velocity range was very narrow [27] or the geometry of the collision [22,28], i.e., the angle of relative approach, was maintained at zero. Our aim is to increase flexibility for both parameters. The experimental setup we use is shown in Fig. 3 and is essentially the same as presented in Ref. [37]. It consists of two main units: the "collision unit" is designed to produce collisions of two spheres of arbitrary diameters with adjustable collision geometry: two steel tubes are mounted on micropositioning slides; one of them is allowed to move horizontally and the other vertically, thus allowing for changes of the relative incidence of the two spheres. One sphere is inserted in each tube and held at the end of the latter by a void pump. A manual trigger releases the pressurized air supply, thus expelling the two spheres. After emergence from the tubes the spheres follow a ballistic trajectory before and after collision. The initial motion takes place in the vertical plane containing the axes of the tubes. The "recording unit" is a Ektapro 1000 High-Speed Video System consisting of the camera itself whose focal plane is parallel to the above precollisional plane, an image processing unit, a video monitor, and an image intensifying unit. The collision scene is lightened from the front with two 750 W Lowell DP lights positioned symmetrically on both sides of the camera. Collisions are recorded on a video tape at a rate of 1000 images per second. A varying number of the resulting gray level images, depending on the velocities and sizes of the spheres, are saved and downloaded on a Unix platform for processing. In order to keep the processing time within reasonable limits, this number is usually of the order of 8 to 12 images (but maybe as low as 2 for high velocities) with approximately as many

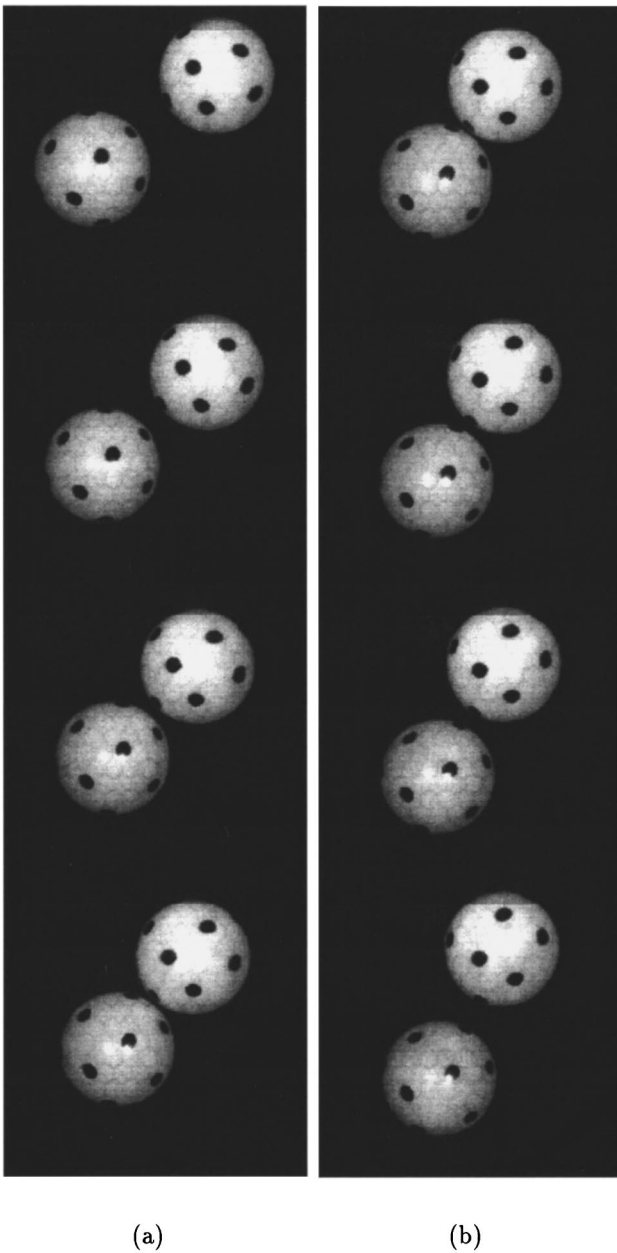


FIG. 4. Sequence of images. Time increases from top to bottom: (a) before collision; (b) after collision.

images before as after collision. Figure 4 shows a sequence of such images. In this particular example images from Fig. 4(a) are taken before collision and those from Fig. 4(b) after collision. The collision takes place within the time interval occurring between the snapshots shown at the bottom of Fig. 4(a) and the top of Fig. 4(b). Edge detection and clustering techniques [31–34] have been implemented to determine the trajectory of the spheres. Once the positions of the centers of the spheres have been determined, we perform a second degree polynomial fit of their respective trajectories, before and after the collision independently. These fits are used to find the “collision time,” i.e., the time when the two trajectories intersect. The velocity components of each sphere before or after the collision are then computed by differentiating the best fits at the “collision time.” The individual spins of the

falling spheres are determined by following the motion, about the sphere centers, of black dots imprinted on their surfaces as shown in Fig. 2. The detection of these markers in the gray level image is performed through a clustering algorithm capable of fitting ellipses [35]. Once the correspondence between markers from one image to the next is known, the position of the markers is shifted to a reference frame connected to the center of the sphere so that only the rotational motion of the markers subsists. The rotation vector from one frame to the next may then be determined by a least squares method as shown in preliminary studies [36,37]. We assume that this rotation does not vary significantly during the recording so that an average rotation vector is computed before and after collision for each sphere. After collision, the velocity components of the spheres perpendicular to the focal plane are then determined from conservation of angular momentum. The ability of this experiment to provide results accurate enough is limited by the resolution of the camera, which is of 192 by 239 pixels. This is why before extracting the features of the images, i.e., the sphere and marker boundaries, a *subpixel* expansion [33] of the image is performed, which is part of the above mentioned “edge detection technique.” This amounts to inserting interpolation points of the intensity of the gray level images, therefore refining the apparent resolution of the camera. The final images have dimensions 4 times larger than the camera resolution, i.e., 768 by 960. Figure 5 shows a gray level image and the detected edge points in the subpixel expansion of this image. The sphere and marker centers are denoted by stars. We verify that this expansion technique actually improves the accuracy. Assuming that the accuracy of the position of a sphere center is of s subpixel units, we may estimate the error made on the measurement of the component of relative velocity \vec{v} in a given direction ξ as

$$\Delta v_{\xi} = \frac{sd}{n_s \delta t \sqrt{N}}, \quad (8)$$

where δt is the average time between two consecutive frames, n_s is the number of subpixels per diameter, and the factor \sqrt{N} (N is the average number of frames before or after collision) is included in a statistical sense to account for the decrease of the standard deviation of our measurements with the increasing number of frames used for a fit. In a series of test collision experiments with 25.4 mm nylon spheres, we measured the Δv_{ξ} from the difference in total momentum of the two spheres, before and after the collision in both directions. If $v_{1\xi}$ and $v_{2\xi}$ are the velocity components of two colliding spheres in either the x or y direction before collision with a prime after collision, we computed Δv_{ξ} as $\Delta v_{\xi} = \frac{1}{2}(v'_{1\xi} + v'_{2\xi} - v_{1\xi} - v_{2\xi})$. Using Eq. (8) where s is now considered as a parameter, we find $s = 1 \pm 0.5$. We conservatively conclude that the subpixel expansion technique guarantees an effective accuracy of 2 subpixels or half a pixel of the initial image. In the conditions of the test experiments, this corresponds to about a 4% uncertainty for measurements of velocities of the order of 1 m s^{-1} .

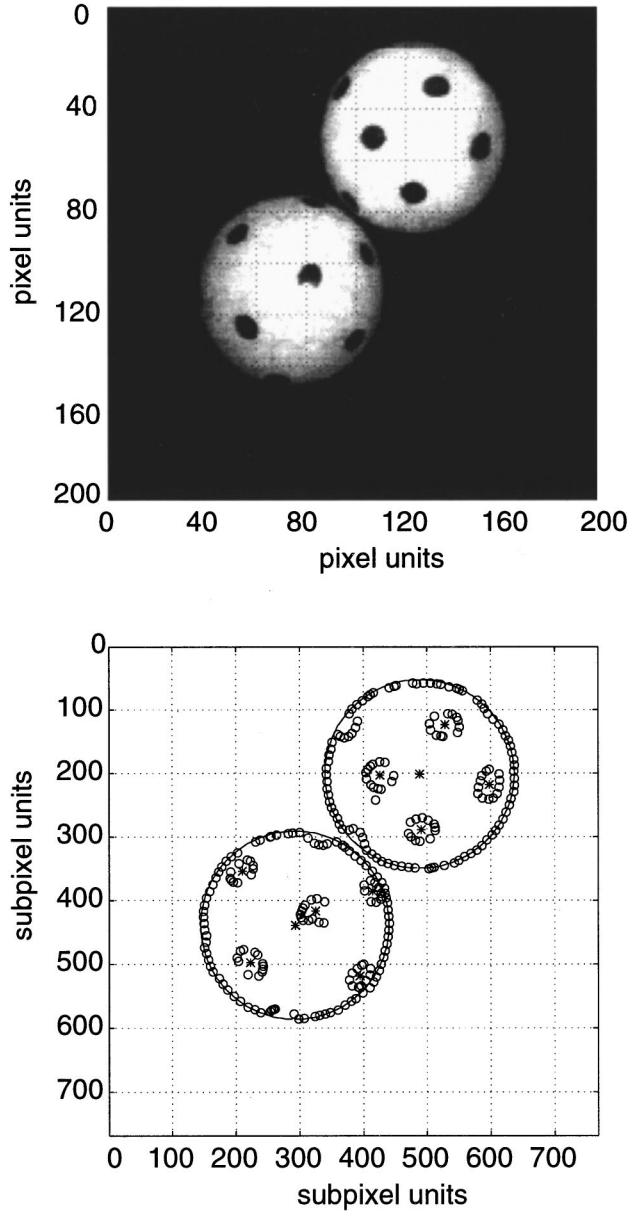


FIG. 5. Gray level image (top) and corresponding *edge* image obtained after processing. The circles are edge points and the stars are the centers of the detected clusters (sphere or marker boundary). Graduations indicate pixel units in the top image and subpixel units in the bottom image.

IV. RESULTS AND DISCUSSION

In order to extract collisional properties at moderate velocities (2 m s^{-1}), we perform a series of experiments with 2.54 cm nylon spheres with a constant release pressure so that the velocity of the spheres at emergence from the tubes is approximately constant. The direction of approach of the spheres is varied by moving the tubes on their respective slides. Figure 6 shows the coefficient of tangential restitution β versus the cotangent of the angle of incidence, $-v_n/v_s$. On this plot we observe the qualitative behavior predicted by Walton's model: for low values of $-v_n/v_s$, β first increases linearly until it reaches a maximum positive value $\beta_0 = 0.5 \pm 0.1$. The average coefficient of normal restitution

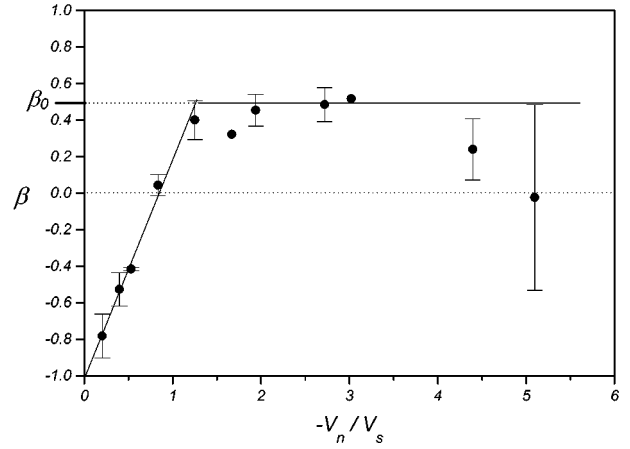


FIG. 6. Coefficient of tangential restitution β vs the cotangent of the angle of incidence.

is found to be over all these collisions $e = 0.97 \pm 0.07$. From the slope of the linear part we can extract $\mu_0 = 0.175 \pm 0.1$. Due to the discrete nature of the video images, the relative error obtained on e increases with decreasing velocity: in fact for $v_n \approx 1 \text{ m s}^{-1}$ we measure $e = 0.97 \pm 0.03$. The overall uncertainty found on e may therefore be interpreted as the signature of the velocity dependence of the coefficient of restitution, consistently with other measurements presented below. Interestingly, we also note that the only two other measurements of β_0 we found in the literature [27] were very close to the value just obtained: 0.43 for soda lime glass spheres and 0.44 for cellulose acetate spheres. We observe, in spite of the increasing uncertainty for large values of $-v_n/v_s$, a tendency of β to decrease from its maximum value β_0 as predicted by Maw *et al.* [23,24].

In another series of experiments we now investigate the mass and velocity dependences of the coefficient of restitution e . In this case the tubes are kept at the same height so that at high velocities the angle of incidence γ of the spheres will be close to π . The pressure is varied to obtain different impact velocity magnitudes. The experiment is performed on nylon spheres with diameters 25.4, 12.7, and 6.35 mm. Results are shown in Fig. 7. Some error bars are shown that are

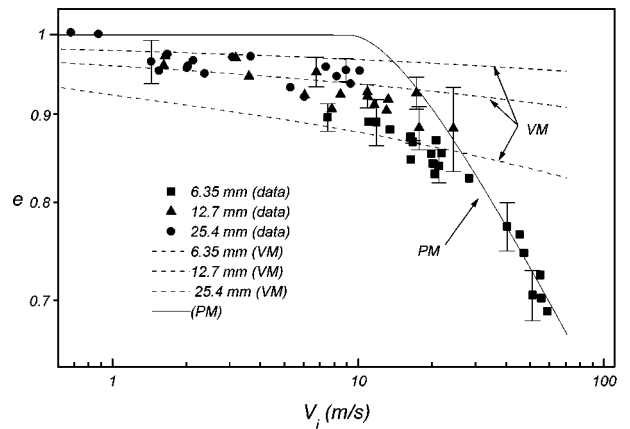


FIG. 7. Coefficient of restitution vs normal impact velocity for nylon spheres for different diameters on a log-log scale. The diameter of the spheres is shown in the figure. VM denotes the viscoelastic model. PM denotes plastic model.

estimated from the change of total momentum as explained earlier, according to

$$\frac{\Delta \epsilon}{\epsilon} \approx 2 \frac{\Delta v_n}{v_n}.$$

It can be observed that the general trend is a decrease of the coefficient of restitution from values close to 1 as the velocity increases. On the other hand, although the results appear quite scattered, there is an aggregation of points according to size, indicating larger values of e , i.e., less dissipation, for larger spheres at fixed velocity. This result is very encouraging and allows us to compare with existing theoretical models of dissipation during collisions. At relatively low speeds, a few meters per second, as used here, energy dissipation appears due to either viscoelasticity of the materials or plastic deformation if, in some region close to the contact surface, the local stress exceeds a typical yield stress or even fracture. It is very likely that in real collisions both viscoelastic and plastic behaviors will come into play and that viscoelastic effects will prevail for small deformations, i.e., small impact velocities. Both behaviors have been modeled theoretically: Kuwabara *et al.* [22] proposed a model of viscoelastic effects based on Hertz's theory [26]. It was compared with experimental measurements made through collisions of two pendula and showed good agreement for materials with the highest restitution or for low impact velocities, typically below 1 m s^{-1} . Johnson [21] proposed a model of plastic dissipation and obtained, in the large velocity limit, an asymptotic behavior in which the coefficient of restitution does not depend on the size of the object and decreases as the power $-1/4$ of the velocity at high velocities. This prediction has been verified experimentally in the case of a sphere impinging a flat plate [28]. We compare our measurements of e with both predictions. In the viscoelastic model, the force P acting between two grains is the sum of an elastic interaction given by Hertz's theory (see Appendix A) and of a viscoelastic force describing the internal friction of the material. The "frictional pressure" is assumed to be proportional to the rate of displacement (i.e., spring and dashpot in parallel):

$$P = \underbrace{2\eta d \dot{\delta} \left(\frac{\delta}{d}\right)^{\frac{1}{2}}}_{\text{viscoelastic damping force}} + \underbrace{Ed^2 \left(\frac{\delta}{d}\right)^{\frac{3}{2}}}_{\text{Hertzian elastic force}} \quad (9)$$

where $E = Y/[3(1 - \nu^2)]$ (Y is modulus of elasticity and ν Poisson's ratio) and η is a phenomenological constant rendering the internal friction of the material. The time evolution of the interparticle "penetration" δ , i.e., the distance of relative approach of the sphere centers during the collision [$\delta = (\vec{r}_1 - \vec{r}_2 - 2R\vec{n}) \cdot \vec{n}$], therefore obeys the following differential equation:

$$m_{\text{red}} \ddot{\delta} = P, \quad (10)$$

where m_{red} is the reduced mass of the two spheres, as in Sec. II. While the value of E is imposed by mechanical properties of the material (Y and ν), we have no information on what η values should be, it may therefore be considered as a fitting

parameter. Equations (9) and (10) were shown in Ref. [38] to yield, in the low dissipation limit, a coefficient of restitution e obeying approximately

$$1 - e \propto \frac{\eta \rho^{2/5}}{E^{-3/5} R} V_i^{1/5}, \quad (11)$$

where V_i is the impact velocity, $R = d/2$ the sphere radius. The size dependence in this model is therefore very strong. We solve this equation numerically over the time interval where $\delta > 0$, i.e., when the spheres are in contact, to compute the coefficient of restitution e . η was chosen so as to grossly center three curves obtained from Eq. (10) at a location satisfactory to the eye. We used the following values of Y and ν : $Y \approx 3.5 \times 10^8 \text{ N m}^{-2}$, $\nu \approx 0.3$, and $\eta \approx 190 \text{ kg s}^{-1} \text{ m}^{-1}$. The mass density for nylon is $\rho \approx 1.14 \times 10^3 \text{ kg m}^{-3}$. The lines labeled "VM" in Fig. 7 are the results thus obtained from Eq. (10) for the three diameters employed: this comparison tells us that the size dependence ($1 - e \propto 1/R$) predicted by Eq. (10) appears to be overestimated (a variation according to $1 - e \propto 1/R^{1/2}$ would be more compatible); the rate of decrease of e with velocity is, however, qualitatively compatible with our measurements. As mentioned earlier, Kuwabara and Kono found that their model was adequate for velocities close to or smaller than 1 m s^{-1} . With our apparatus probing such a low velocity range becomes somewhat awkward and the discrepancy of our data with the viscoelastic model may well be due to the fact that we used velocities above its range of validity.

For the smallest spheres and velocities larger than about 25 m s^{-1} , the experimental data clearly plummet below the VM prediction, possibly indicating the occurrence of a different dissipation mechanism. In this velocity range we do not have any data for the larger sizes. However, this deviation incites us to compare our data with a model for plastic deformation since we expect that plasticity has to come into play. In order to extend Johnson's prediction to intermediate values of V_i , we follow Ning and Thornton [39]. In their model, as long as no plastic deformation occurs, the contact force is given by Hertz's theory, i.e.,

$$P(\delta) = Ed^2 \left(\frac{\delta}{d}\right)^{1/2}.$$

If plastic deformation occurs the pressure distribution is Hertzian across the contact surface, which is a disk of radius a such that $2a^2 = R\delta$, with a cutoff at a specified value of yield stress σ_y . In other words, when the maximum elastic stress experienced by the spheres during an elastic impact as given by Hertz reaches σ_y , a central plastic disk develops inside the contact patch, where the pressure saturates at the cutoff stress σ_y . In the remaining part of the contact zone, the pressure profile is assumed to follow Hertz's theory. The pressure increases from zero at the boundary of the contact patch to σ_y at the boundary of the inner plastic disk. The resulting force-displacement relationship after yield has been reached becomes linear [see Eq. (12) below]. For details on the exact signification of σ_y see, for example, Ref. [21]. We did not take into account any variation of the contact curvature, as was done in Ref. [39], in this region during the elastic-plastic loading but instead kept it constant equal to

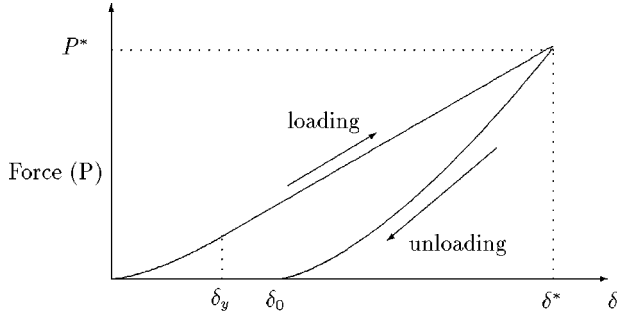


FIG. 8. Force displacement curve for the elastic-plastic model given by Eqs. (12) and (13).

the initial curvature. A calculation similar to that of Ref. [39] gives the repulsive force between the two spheres during loading:

$$P_{\text{loading}}(\delta) = \begin{cases} Ed \left(\frac{\delta}{d} \right)^{1/2} \delta & \text{for } \delta \leq \delta_y \\ \frac{1}{2} \pi \sigma_y R (\delta - \delta_y) + Ed \left(\frac{\delta_y}{d} \right)^{1/2} \delta_y & \text{for } \delta_y \leq \delta \leq \delta^* \end{cases} \quad (12)$$

where δ_y (see Appendix B) is the penetration for which the maximum pressure first reaches σ_y and δ^* is the maximum penetration, corresponding to the end of loading. Unloading is done elastically with a larger contact curvature R' so that the elastic force comes to zero after an elastic displacement ($\delta^* - \delta_0$) smaller than δ^* , that achieved during loading:

$$P_{\text{unloading}}(\delta) = \frac{2^{1/2} E}{R'} [R' (\delta - \delta_0)]^{3/2} \quad \text{for } \delta_0 \leq \delta \leq \delta^*. \quad (13)$$

Both the new curvature and the ‘‘permanent indentation,’’ δ_0 , stem directly from the continuity of the maximum force P^* and of the radius of the contact area at the end of the loading phase, i.e.,

$$\begin{aligned} P_{\text{loading}}(\delta^*) &= P_{\text{unloading}}(\delta^*), \\ R' (\delta^* - \delta_0) &= R \delta^* = 2a^{*2}. \end{aligned} \quad (14)$$

A discontinuity of the curvature thus arises that may be regarded as a discontinuity of the average curvature between the loading and unloading phases. The force-displacement curve $P(\delta)$ is shown in Fig. 8. Yield first occurs when the stress as predicted by Hertz’s theory at the center of the contact patch reaches σ_y . This happens if the initial impact velocity is larger than the ‘‘yield velocity’’ V_Y given by (see Appendix B)

$$V_Y = \frac{1}{9\sqrt{10}} \left(\frac{\pi^4 \sigma_y^5}{\rho E^4} \right)^{1/2}. \quad (15)$$

The relative approach of the sphere centers is then $\delta = \delta_y = (1/18) \pi^2 R (\sigma_y/E)^2$. For $V_i \leq V_Y$, no dissipation occurs, i.e., $e = 1$. For $V_i \geq V_Y$, we compute the coefficient of

restitution by comparison between the work done by the repulsive force P during the loading and unloading phases. The work done until the instant of maximal compression is

$$W_i = \frac{1}{2} m_{\text{red}} V_i^2 = \int_0^{\delta^*} P d\delta. \quad (16)$$

During rebound, the work done by the elastic force is

$$W_r = \frac{1}{2} m_{\text{red}} V_r^2 = \frac{P^{*2}}{5Ea^*}. \quad (17)$$

From Eqs. (16) and (17), an exact solution may be found for the coefficient of restitution $e = (W_r/W_i)^{1/2}$. This expression yields an asymptotic limit for $V_i \gg V_Y$ in agreement with Johnson’s:

$$e \approx 1.18 \left(\frac{V_i}{V_Y} \right)^{-1/4}. \quad (18)$$

The solution is plotted on Fig. 7 with the label ‘‘PM’’ and gives a very good agreement for the smallest spheres, showing the existence of a crossover region between viscoelastic and plastic behaviors for velocities around 10 m s^{-1} . We used $\sigma_y \approx 4.0 \times 10^7 \text{ N/m}^2$, for which the yield velocity is $V_Y \approx 9 \text{ m s}^{-1}$. This plastic model defines a ‘‘universal curve’’ with no size dependence. More data for the larger sizes are needed, however, to confirm the predicted scaling of e .

V. CONCLUSION

An experimental apparatus was designed to perform measurements of sphere collision properties: these properties characterize in a quantitative way the impact of two granules and therefore can be used to check the relevance of a given force scheme or collision operator used in computer simulations or theoretical studies for a given material. This kind of measurement is of crucial importance to physicists dealing with modeling of rapid flows of granular materials. These properties are extracted by using a collision operator as was previously done in [23,27]. In this model the possibility of retrieving part of the elastic energy stored in the early moments of a collision where sticking is involved, responsible for the reversal of the relative surface velocity, is measured by the coefficient β_0 , which was found to be very close to previous values obtained for other materials [27]. With this experimental setup we were able to provide results on the size and mass dependence of the coefficient of restitution for the collision of spheres in free flight and to test the relevant dissipation hypotheses. It appears first that there is a range of velocities in which the coefficient of restitution decreases as the size of the objects decreases. In this range we compared our data with a model of viscoelastic dissipation [22] and showed that the size dependence in this model was overestimated but that the velocity dependence $(1 - e \propto V_i^{0.2})$ gave a good order of magnitude of the rate of decrease of e with V_i . As the velocity increased we showed that the viscoelastic assumption was no longer valid and that the stronger dissipation regime (smaller e) was very well described by a model of plastic deformation inspired from [21,39]. Unfor-

tunately we could not check the size independence predicted by this model due to limitations of the experimental setup. Finally our results show that both models bear some relevance to the dissipation processes involved according to the velocity range used and that the yield velocity V_Y given by the plastic model is a good indicator of the crossover between the two dissipation regimes. The observed discrepancy of our data compared with the viscoelastic model may be due to the fact that the velocity range we can probe is above the range of validity of the model (in which a linear relationship is assumed between “frictional pressure” and rate of displacement) for this material. This experimental device proved to be a suitable apparatus to give quantitative information concerning the collision of inelastic frictional spheres in relevance to the physics of granular media.

ACKNOWLEDGMENTS

This work was supported through a National Science Foundation (NSF) Combined Research and Curriculum Development grant (EEC-94200597) and through an NSF equipment grant (MSS-9006822). We thank Eric Clément for helpful discussions and critical comments on this manuscript.

APPENDIX A: COMPRESSION OF TWO ELASTIC SPHERES (HERTZ)

We briefly recall results established by Hertz in 1890 (see, for example, [21] or [26]), which predict the deformation of two elastic spheres pressed together by a force $\vec{P} = P\vec{u}_z$ where \vec{u}_z is a unit vector parallel to the line joining their centers. The results were established for spheres of arbitrary radii R_1 and R_2 , Young’s moduli Y_1 and Y_2 , and Poisson’s ratios ν_1 and ν_2 . The two spheres are in contact across a circular surface of radius $a(P)$. From symmetry arguments, the only nonzero stress component is that parallel to the direction of the applied force:

$$\sigma_{zz}(r) = \frac{3P}{2\pi a^3} (a^2 - r^2)^{1/2}, \quad (\text{A1})$$

where r is the radial coordinate measured from the center of the contact surface. The radius of the contact area is related to the distance of relative approach δ through

$$\tilde{R}\delta = a^2.$$

The force P is

$$P = \int_0^a 2\pi r \sigma(r) dr = \frac{4\tilde{E}}{R} a^3 = 4\tilde{E}\tilde{R}^2 \left(\frac{\delta}{\tilde{R}}\right)^{3/2}, \quad (\text{A2})$$

where

$$\frac{1}{\tilde{E}} = \frac{3(1-\nu_1^2)}{Y_1} + \frac{3(1-\nu_2^2)}{Y_2}$$

and

$$\frac{1}{\tilde{R}} = \frac{1}{R_1} + \frac{1}{R_2}.$$

APPENDIX B: COMPLEMENTS ON SOME RESULTS OF SECTION IV

In the case of identical spheres (same size and material), the elastic force given in Eq. (A2) reduces to

$$P = E d^2 \left(\frac{\delta}{d}\right)^{3/2}. \quad (\text{B1})$$

Plastic deformation first occurs when $\sigma_{zz}(r=0) = \sigma_y$. Using Eqs. (B1) and (A1), this gives a relationship between the penetration δ_y at initial yield and σ_y :

$$\delta_y = \frac{\pi^2}{18} \left(\frac{\sigma_y}{E}\right)^2 R. \quad (\text{B2})$$

The yield velocity is obtained from a balance between the initial kinetic energy and the work done by the elastic force during loading up to the onset of yield:

$$\frac{1}{2} m_{\text{red}} V_Y^2 = \int_0^{\delta_y} P d\delta. \quad (\text{B3})$$

Equations (B3) and (B2) and the first of Eqs. (12) are combined to find the yield velocity in Eq. (15).

[1] H. M. Jaeger and S. R. Nagel, *Science* **255**, 1523 (1992); H. M. Jaeger, J. B. Knight, C. H. Liu, and S. R. Nagel, *MRS Bull.* **5**, 25 (1994).
 [2] P. A. Cundall and O. D. L. Strack, *Geotechnique* **29**, 47 (1979).
 [3] S. Luding, E. Clément, A. Blumen, J. Rajchenbach, and J. Duran, *Phys. Rev. E* **50**, R1762 (1994).
 [4] S. Luding, *Phys. Rev. E* **52**, 4442 (1995).
 [5] Y.-h. Taguchi, *Phys. Rev. Lett.* **69**, 1371 (1992).
 [6] J. A. C. Gallas, H. J. Herrmann, and S. Sokołowski, *Phys. Rev. Lett.* **69**, 1375 (1992).
 [7] S. Luding, E. Clément, A. Blumen, J. Rajchenbach, and J.

Duran, *Phys. Rev. E* **50**, 4113 (1994).
 [8] O. R. Walton and R. L. Braun, *J. Rheol.* **30**, 949 (1986); O. R. Walton, in *Particulate Two Phase Flow*, edited by M. C. Roco (Butterworth-Heinemann, Boston, 1992), pp. 884–907.
 [9] S. Luding, E. Clément, A. Blumen, J. Rajchenbach, and J. Duran, *Phys. Rev. E* **49**, 1634 (1994).
 [10] S. Luding, H. J. Herrmann, and A. Blumen, *Phys. Rev. E* **50**, 3100 (1994).
 [11] R. Mazighi, B. Bernu, and F. Delyon, *Phys. Rev. E* **50**, 4551 (1994).
 [12] B. Bernu and R. Mazighi, *J. Phys. A* **23**, 5745 (1990).
 [13] M. P. Allen and D. J. Tildesley, *Computer Simulation of Liq-*

- uids* (Oxford University Press, Oxford, 1987).
- [14] B. D. Lubachevsky, *J. Comput. Phys.* **94**, 255 (1991).
- [15] S. McNamara and W. R. Young, *Phys. Fluids A* **4**, 496 (1992).
- [16] S. McNamara and W. R. Young, *Phys. Fluids A* **5**, 34 (1993).
- [17] Y. Du, H. Li, and L. P. Kadanoff, *Phys. Rev. Lett.* **74**, 1268 (1995).
- [18] O. R. Walton, *Acta Mech.* **63**, 947 (1986).
- [19] M. H. Sadd, Q. Tai, and A. Shukla, *Int. J. Non-Linear Mech.* **28**, 251 (1993).
- [20] J. Schäfer, S. Dippel, and D. E Wolf, *J. Phys. I* **6**, 5 (1996).
- [21] K. L. Johnson, *Contact Mechanics* (Cambridge University Press, New York, 1985).
- [22] G. Kuwabara and K. Kono, *Jpn. J. Appl. Phys.* **26**, 1230 (1987).
- [23] N. Maw, J. R. Barber, and J. N. Fawcett, *Wear* **38**, 101 (1976).
- [24] N. Maw, J. R. Barber, and J. N. Fawcett, *J. Lub. Tech. (Trans ASME)* **20**, 327 (1981).
- [25] N. V. Brilliantov, F. Spahn, J.-M. Hertzsch, and T. Pöschel, *Phys. Rev. E* **53**, 5382 (1996).
- [26] L. D. Landau and E. M. Lifshitz, *Theory of Elasticity* (Pergamon Press, London, 1959).
- [27] S. F. Foerster, M. Y. Louge, H. Chang, and K. Allia, *Phys. Fluids* **6**, 3 (1994).
- [28] W. Goldsmith, *Impact* (E. Arnold Publications, London, 1960).
- [29] R. Sondergard and K. Chaney, *J. Appl. Mech.* **57**, 694 (1990).
- [30] R. D. Mindlin, *J. Appl. Mech.* **16**, 259 (1949); R. D Mindlin and H. Deresiewicz, *ibid.* **21**, 237 (1953).
- [31] S. McNamara and W. R. Young, *Phys. Rev. E* **50**, R28 (1994).
- [32] J. A. C. Gallas, H. J. Herrmann, and S. Sokołowski, *Physica A* **189**, 437 (1992).
- [33] A. Huertas and G. Medioni, *IEEE Trans. Pattern. Anal. Mach. Intell.* **8**, 651 (1986).
- [34] J. Illingworth and J. Kittler, *IEEE Trans. Pattern. Anal. Mach. Intell.* **5**, 690 (1987).
- [35] R. N. Dave and K. Bashwan, *IEEE Trans. Neural Netw.* **3**, 643 (1992).
- [36] J. Yu, M.S. thesis, NJIT, Newark, NJ (1993).
- [37] R. N. Dave, J. Yu, and A. D. Rosato (unpublished).
- [38] S. Luding, Ph.D. dissertation, University of Freiburg, Germany (1994).
- [39] Z. Ning and C. Thornton, in *Powders & Grains 93*, edited by C. Thornton (Balkema, Rotterdam, 1993).